Constraining Neutron-Star Matter — Combination of heavy-ion experiments, astronomy and theory.

Arnaud Le Fèvre[8*], *Sabrina* Huth[1,2,13], *Peter T. H.* Pang[3,4,13], *Ingo* Tews[5], *Tim* Dietrich[6,7], *Achim* Schwenk[1,2,9], *Wolfgang* Trautmann[8], *Kshitij* Agarwal[10], *Mattia* Bulla[11], *Michael W.* Coughlin[12] and *Chris* Van Den Broeck[3,4]

[1]Department of Physics, Technische Universität Darmstadt, Darmstadt, Germany.
[2]ExtreMe Matter Institute EMMI, GSI Helmholtzzentrum für Schwerionenforschung GmbH, Darmstadt, Germany.
[3]Nikhef, Amsterdam, The Netherlands.
[4]Institute for Gravitational and Subatomic Physics (GRASP), Utrecht University, Utrecht, The Netherlands.
[5]Theoretical Division, Los Alamos National Laboratory, Los Alamos, NM, USA.
[6]Institut für Physik und Astronomie, Universität Potsdam, Potsdam, Germany.
[7]Max Planck Institute for Gravitational Physics (Albert Einstein Institute), Potsdam, Germany.
[8]GSI Helmholtzzentrum für Schwerionenforschung GmbH, Darmstadt, Germany.
[9]Max-Planck-Institut für Kernphysik, Heidelberg, Germany.
[10]Physikalisches Institut, Eberhard Karls Universität Tübingen, Tübingen, Germany.
[11]The Oskar Klein Centre, Department of Astronomy, Stockholm University, AlbaNova, Stockholm, Sweden.
[12]School of Physics and Astronomy, University of Minnesota, Minneapolis, MN, USA.

Abstract. Interpreting high-energy, astrophysical phenomena, such as supernova explosions or neutron-star collisions, requires a robust understanding of matter at supranuclear densities. However, our knowledge about dense matter explored in the cores of neutron stars remains limited. Fortunately, dense matter is not probed only in astrophysical observations, but also in terrestrial heavy-ion collision experiments. In a novel approach, using Bayesian inference, we combine data from astrophysical multi-messenger observations of neutron stars [1-9] and from heavy-ion collisions at relativistic energies [10,11] with microscopic nuclear theory calculations [12-17] to improve our understanding of dense matter. We find that the inclusion of heavy-ion collision data indicates an increase in the pressure in dense matter relative to previous analyses, shifting neutron-star radii towards larger values, consistent with recent observations by the Neutron Star Interior Composition Explorer mission [5-8,18]. It is found in addition that constraints from heavy-ion collision experiments show a remarkable consistency with multi-messenger observations and provide complementary information on nuclear matter at intermediate densities. This work combines nuclear theory, nuclear experiment and astrophysical observations, and shows how joint analyses can shed light on the properties of neutron-rich supranuclear matter over the density range probed in neutron stars. (Work primarily published in Ref. [44]: S. Huth, et al., Nature 606 (2022)).

1 Introduction

The nuclear equation of state (EOS) describes dense matter probed in terrestrial experiments with atomic nuclei as well as in astrophysical observations of neutron stars. The nuclear EOS has to be determined through approximate theoretical calculations or from experimental or observational data. As a result, at densities well above nuclear saturation density, n_{sat} = 0.16 fm^{-3}, for which experimental and theoretical information are less robust, the nuclear EOS is still highly uncertain and many open questions remain, such as whether a possible phase transition to exotic phases of matter exists in nature [19].

At densities below 1–2n_{sat}, the EOS and its theoretical uncertainty can be obtained from microscopic calculations based on chiral effective field theory (EFT) of QCD [12–17]. To probe dense matter beyond these densities, further approaches, based on experimental and observational data, are necessary. A very promising tool is the multi-messenger astrophysics analysis of neutron stars and their collisions, which provides access to dense neutron-rich matter not accessible in terrestrial experiments at present. In recent years, the advent of gravitational-wave (GW) astronomy [1] and new electromagnetic observations of neutron stars [3,5,6], including the Neutron Star Interior Composition Explorer (NICER) mission of the National Aeronautics and Space Administration (NASA) [5,6], led to new constraints on the EOS [7,9,18,20–26]. However, these observations mainly probe the EOS at densities $\gtrsim 2n_{sat}$ and still carry considerable uncertainties, reflected in the ranges for predictions of neutron-star radii. More precise or new complementary information is required to reduce the uncertainties further.

The gap between our current knowledge of the EOS stemming from nuclear theory and experiment at low densities and astrophysical observations of neutron stars at higher densities can be bridged by heavy-ion collision (HIC) experiments. These experiments, performed with heavy-ion beam energies of up to 2 GeV per nucleon, probe the nuclear EOS mainly in a

* Corresponding author: a.lefevre@gsi.de

density range of 1–2n_{sat} at present [10,11,27], representing a new source of information [28].

2 Method.

In this work, within a Bayesian multimessenger framework [9,39], which analyses each EOS with respect to its agreement with a variety of observational data, we have combined information from nuclear theory (Fig. 1a), astrophysical observations of neutron stars (Fig. 1b) and results from HIC experiments (Four-Pi (FOPI) [10] and the Asymmetric-Matter EOS (ASY-EOS) experimental campaigns [11]) that were performed at the GSI Helmholtz Centre for Heavy Ion Research (Fig. 1c). The combination of these experiments provides new constraints for neutron-rich matter in the range around 1–2n_{sat}. The EOS constraint from ref. 27 for symmetric nuclear matter obtained from HIC experiments at the Bevalac accelerator at Lawrence Berkeley National Laboratory and the Alternating Gradient Synchrotron at Brookhaven National Laboratory has been included as well. In all experiments, gold nuclei were collided. The information from this series of HIC experiments allows us to further constrain the EOS in a density range for which theoretical calculations become less reliable.

3 Nuclear theory input

15,000 EOS's have been sampled for the local chiral effective field theory (EFT) interactions [14,29-31] to build the prior set of the Bayesian analysis. The EFT expansion enables estimates of theoretical uncertainties [16,32] needed by the Bayes method. The local chiral two- and three-nucleon interaction Monte-Carlo sampling of the chiral-EFT are among the most precise many-body methods to solve the nuclear many-body problem [33]. The breakdown scale of the expansion was estimated to be about 500–600 MeV/c [16]. Therefore, the EOS set using chiral EFT input has been limited only up to 1.5n_{sat} (corresponding to Fermi momenta of the order of 400 MeV/c), but a variation in the range 1–2n_{sat} has shown no substantial impact on our final results for neutron-star radii [34]. Above the 1.5n_{sat} limit, each EOS is extrapolated according to the speed of sound (c_s) in neutron-star matter [35], constrained only by causality ($c_s \leq c$) and stability of neutron-star matter ($cs \geq 0$). No information at asymptotically high densities from perturbative QCD calculations is taken into account. In addition, selected EOSs support neutron stars with masses of at least 1.9 solar masses (1.9$M_\odot$). EOSs that support only neutron stars with maximum masses well below the lower limit from the combined observations of heavy pulsars [36–38] are removed from the sample.

These general assumptions lead to a broad uncertainty for the EOS at higher densities (Fig. 1a), as well as for neutron-star masses and radii (Fig. 2a of Ref. [44]). The EOS prior is then used to analyse astrophysical observations and HIC experiments.

4 Multi-messenger astrophysics information

Various constraints from multi-messenger astronomy observations have been applied to the Bayesian analysis, with following sequence of constraints: (1) The lower and upper bounds of the maximum mass of neutron stars, respectively constrained by measurements of massive neutron stars (pulsars) PSR J0348+0432 [36] and PSR J1614-2230 [37] on the one side, and from the observation of the binary neutron-star collision GW170817 [40,41] on the other side. (2) Constraints from X-ray pulse-profile modelling of PSR J0030+0451 and PSR J0740+6620 using data from NICER and the X-ray Multi-Mirror Mission (XMM-Newton) [5,7,8]. (3) GW information from the two neutron-star mergers GW170817 [1] and GW190425 [2] by matching the observed GW data with theoretical GW models that depend on neutron-star properties [42], using an improved version of the main waveform model used by the Laser Interferometer Gravitational-Wave Observatory/Virgo Collaboration for the study of GW170817 [43] and GW190425 [2]. (4) Information from the kilonova AT2017gfo [3] associated with the GW signal. Fig. 1b shows that the above astrophysical informations leads to important constraints on the neutron-star EOS. The effect is strongest above 1.5n_{sat}, where the extrapolation in the speed of sound is used for the EOSs of the prior. The high-density astrophysical constraints affect mostly the high-mass region in the mass–radius plane and exclude the stiffest EOSs that lead to the largest radii (Fig. 2b of Ref. [44]).

5 Data from HIC experiments

As a last layer of constraints in the Bayesian analysis, the EOS constraint from HIC experiments has been applied. The FOPI [10] and ASY-EOS [11] experiments performed at GSI provide information respectively on the symmetric nuclear matter EOS (that is, matter with the same amount of protons and neutrons) and on the symmetry energy, which describes the energy cost of changing protons into neutrons in nuclear matter. For both experiments,

^{197}Au nuclei were collided at relativistic energies (0.4 to 1.5 GeV per nucleon), forming an expanding fireball in the collision region. This expansion is dictated by the achieved compression and therefore depends on the EOS of hot and dense matter. Owing to the initial neutron-to-proton asymmetry of the Au–Au system, the expansion of the emitted nucleons is sensitive to the nuclear symmetry energy. Constraints on the symmetry energy (from ASY-EOS) can be translated into a constraint on the pressure of neutron-star matter as a function of the baryon density when empirical information on symmetric nuclear matter from experiments (FOPI) with atomic nuclei is used. Whereas the FOPI experiment delivers an EOS constraint for symmetric nuclear matter at densities in the range 1–3n_{sat}, the ASY-EOS experiment probes the symmetry energy roughly between 1 and 2n_{sat}. Additional constraints on the pressure of symmetric nuclear matter have been applied at larger densities, obtained from experimental data from Lawrence Berkeley National Laboratory and Brookhaven National Laboratory [27] in which ^{197}Au nuclei were collided at energies up to 10 GeV per nucleon. These are sensitive to higher densities, 2–4.5n_{sat}, but we include their constraints only up to 3n_{sat}, where the sensitivity of the ASY-EOS experiment ends. We find that the inclusion of this further constraint has only minimal impact. Fig. 1c shows that the combined HIC experimental constraints for the neutron-star EOS tend to prefer EOSs stiffer than the ones favored by astrophysical observations (that is, EOSs that have higher pressures at densities up to 2n_{sat}; Figs. 1c, 2a).

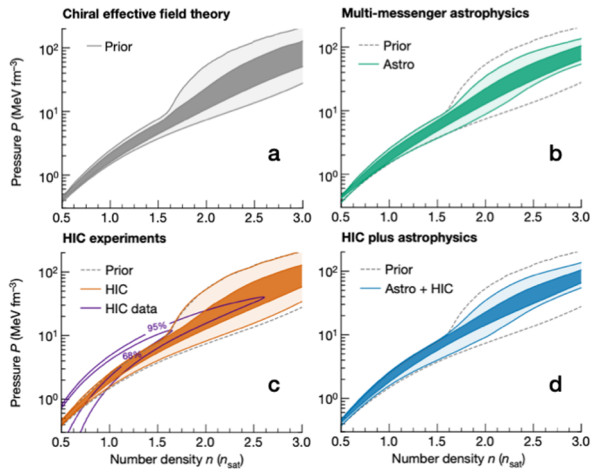

Fig. 1. Constraints on the EOS of neutron-star matter. a–d, Evolution of the pressure as a function of baryon number density for the EOS prior (a, grey), when including only data from multi-messenger neutron-star observations (b, green), when including only HIC data (c, orange), and when combining both (d, blue). The shading corresponds to the 95% and 68% credible intervals (lightest to darkest). The impact of the HIC experimental constraint (HIC data, purple lines at 95% and 68%) on the EOS is shown in c. In b–d, the 95% prior bound is shown for comparison (grey dashed lines).

6 Combining microscopic and macroscopic collisions

The final EOS constraints are obtained through the combination of both the HIC information and astrophysical multi-messenger observations (Fig. 1d). The multi-messenger data rule out the most extreme EOS behavior, and the HIC data favor larger pressures around 1–1.5n_{sat}, the density range where the HIC experimental sensitivity is highest. This is similar to the effect of recent NICER observations on the EOS [7,18]. Hence, the two complementary approaches, HIC experiments and astrophysical observations, show a remarkable agreement (Fig. 2a). At low densities, HIC results have a clear impact on the total posterior for the EOS, whereas the EOS at higher densities ($\gtrsim$2n_{sat}) is mostly determined by astrophysical observations. At these densities, HIC results deviate only mildly from the prior (Fig. 2b). This is also reflected in the radii of neutron stars shown in Fig. 2e, f of Ref. [44]. As astrophysical observations mainly probe neutron stars with $M \gtrsim 1.4 M_\odot$, for which the relevant densities are higher, HIC information influences the radii of these neutron stars to a smaller degree. On the other hand, the radius of low-mass stars with $M \approx 1.0 M_\odot$ is also constrained by HIC information. Our final result for a typical $1.4 M_\odot$ neutron star is $12.01^{+0.37}_{-0.38}$ km at 68% uncertainty ($12.01^{+0.78}_{-0.77}$ km at 95% uncertainty). Comparing this value to the result without any HIC information, $11.93^{+0.39}_{-0.41}$ km at 68% confidence, highlights the benefit of combining these various sources of information in a statistically robust framework.

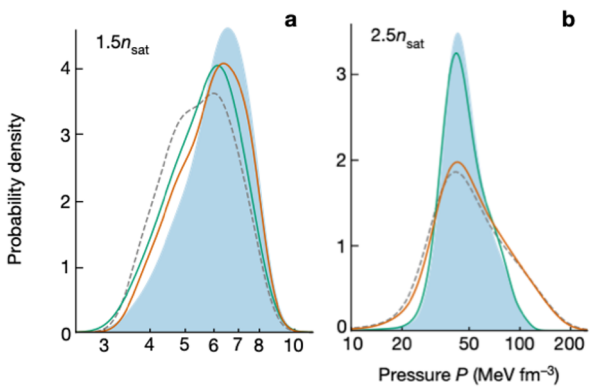

Fig. 2. Posterior distributions for the pressure at 1.5n_{sat} (a) and 2.5n_{sat} (b) at different stages of our analysis, with the combined Astro + HIC region shaded in light blue.

7 Perspectives.

Advancing HIC experiments to probe higher densities, above 2–3n_{sat}, will be key. Combining the latter with a reduction of experimental uncertainties, data from HICs have great potential to provide complementary EOS information, bridging nuclear theory and astrophysical observations. In the next few years, the ASY-EOS-II and Compressed Baryonic Matter experiments at the upcoming Facility for Antiproton and Ion Research at GSI will provide a unique opportunity to study nuclear matter at densities probed in the core of neutron stars and their mergers, and might detect new phases of QCD matter, possibly involving hyperons and, ultimately, the transition to a deconfined quark matter phase at the highest densities. Together with experiments at the Rare Isotope Beam Facility at RIKEN in Japan and the Nuclotron-Based Ion Collider Facility in Russia, the robust combination of experimental

HIC constraints and astrophysical observations has the potential to revolutionize our understanding of the EOS.

References

1. B.P. Abbott, et al., Phys. Rev. Lett. **119**, 161101 (2017).
2. B. Abbott, et al., J. Lett. **892**, L3 (2020).
3. B.P. Abbott, et al., Astrophys. J. **848**, L13 (2017).
4. M. Coughlin, et al., Astrophys. J. **849**, 12 (2017).
5. M. C. Miller et al., Astrophys. J. Lett. **887**, L24 (2019).
6. T.E. Riley, et al., Astrophys. J. Lett. **887**, L21 (2019).
7. M.C. Miller, et al., Astrophys. J. Lett. **918**, L28 (2021).
8. T.E. Riley, et al., Astrophys. J. Lett. **918**, L27 (2021).
9. T. Dietrich, et al., Science **370**, 1450–1453 (2020).
10. A. Le Fèvre, Y. Leifels, W. Reisdorf, J. Aichelin and C. Hartnack, Nucl. Phys. A **945**, 112–133 (2016).
11. P. Russotto, et al., Phys. Rev. C **94**, 034608 (2016).
12. K. Hebeler, J.M. Lattimer, C.J. Pethick and A. Schwenk, Astrophys. J. **773**, 11 (2013).
13. I. Tews, T. Krüger, K. Hebeler, and A. Schwenk, Phys. Rev. Lett. **110**, 032504 (2013).
14. J.E. Lynn, et al., Phys. Rev. Lett. **116**, 062501 (2016).
15. C. Drischler, K. Hebeler, and A. Schwenk, Phys. Rev. Lett. **122**, 042501 (2019).
16. C. Drischler, R.J. Furnstahl, J.A. Melendez, and D.R. Phillips, Phys. Rev. Lett. **125**, 202702 (2020).
17. S. Huth, C. Wellenhofer an A. Schwenk, Phys. Rev. C **103**, 025803 (2021).
18. G. Raaijmakers, et al., Astrophys. J. Lett. **918**, L29 (2021).
19. E. Annala, T. Gorda, A. Kurkela, J. Nättilä and A. Vuorinen, Nat. Phys. **16**, 907–910 (2020).
20. A. Bauswein, O. Just, H.-T. Janka and N. Stergioulas, Astrophys. *J.* **850**, L34 (2017).
21. E. Annala, T. Gorda, A. Kurkela and A. Vuorinen, Phys. Rev. Lett. **120**, 172703 (2018).
22. E.R. Most, L.R. Weih, L. Rezzolla and J. Schaffner-Bielich, Phys. Rev. Lett. **120**, 261103 (2018).
23. B.P. Abbott, et al., Phys. Rev. Lett. **121**, 161101 (2018).
24. D. Radice and L. Dai, Eur. Phys. J. **A55**, 50 (2019).
25. C.D. Capano, et al., Nat. Astron. **4**, 625–632 (2020).
26. I. Legred, K. Chatziioannou, R. Essick, S. Han and P. Landry, Phys. Rev. D **104**, 063003 (2021).
27. P. Danielewicz, R. Lacey, and W.G. Lynch, Science **298**, 1592–1596 (2002).
28. M.B. Tsang, W.G. Lynch, P. Danielewicz, and C.Y. Tsang, Phys. Lett. B **795**, 533–536 (2019).
29. I. Tews, J. Carlson, S. Gandolfi and S. Reddy, Astrophys. J. **860**, 149 (2018).
30. E. Epelbaum, H.-W. Hammer and U.-G. Meissner, Rev. Mod. Phys. **81**, 1773–1825 (2009).
31. R. Machleidt, and D.R. Entem, Phys. Rep. **503**, 1–75 (2011).
32. E. Epelbaum, H. Krebs and U.-G. Meißner, Eur. Phys. J. A **51**, 53 (2015).
33. J. Carlson, et al., Rev. Mod. Phys. **87**, 1067 (2015).
34. R. Essick, I. Tews, P. Landry, S. Reddy, and D.E. Holz, Phys. Rev. C **102**, 055803 (2020).
35. I. Tews, J. Margueron, and S. Reddy, Phys. Rev. **C98**, 045804 (2018).
36. J. Antoniadis, et al., Science **340**, 1233232 (2013).
37. Z. Arzoumanian, al., Astrophys. J. Suppl. Ser. **235**, 37 (2018).
38. E. Fonseca, et al., Astrophys. J. Lett. 915, L12 (2021).
39. P.T.H. Pang, et al., Astrophys. J. 922, 14 (2021).
40. B. Margalit, and B.D. Metzger, Astrophys. J. 850, L19 (2017).
41. L. Rezzolla, E.R. Most, and L.R. Weih, Astrophys. J. 852, L25 (2018).
42. T. Dietrich, et al., Phys. Rev. D 100, 044003 (2019).
43. B.P. Abbott, et al., Phys. Rev. X 9, 011001 (2019).
44. S. Huth, P.T.H. Pang, et al., Nature 606 (2022).